

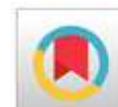


Extracellular biosynthesis of silver nanoparticles using *Bacillus subtilis* and their antibacterial activity against clinical bacterial species

Nouran H. Assar^{1*}; Aya Allah T. Mohamed^{2,3}; Rehab M. Abd El-Baky^{2,3}; Reham Ali Ibrahim²

¹Department of Microbiology, General Division of Basic Medical Sciences, Egyptian Drug Authority former National Organization for Drug Control and Research (NODCAR), Giza, Egypt; ²Department of Microbiology and Immunology, Faculty of Pharmacy, Minia University, Minia, Egypt; ³Microbiology and Immunology Department, Faculty of Pharmacy, Deraya University, Minia, Egypt

*Corresponding author E-mail: drnouranhamed@hotmail.com



Received: 17 May, 2021; Accepted: 15 June, 2021; Published online: 17 June, 2021

Abstract

The aims of this study were to biosynthesize silver nanoparticles (AgNPs) using *Bacillus subtilis* supernatant, and to evaluate their *in vitro* antibacterial potential against human pathogens; namely *Staphylococcus aureus* (*Staph. aureus*) and *Escherichia coli* (*E. coli*). Nanoparticles (NPs) are becoming popular in different fields of research, and are useful in combating vast number of microbial diseases. NPs may be artificially synthesized *in vitro* using chemical methods and/or via extracellular metabolites produced by the bacterial strains. In the present study, biosynthesis of AgNPs was carried out *in vitro* using supernatants of *B. subtilis*. Biosynthesized AgNPs were characterized through several physical methods. The recorded Z-average (d. nm) was 135.0 nm; with 99.2 % of the NPs displaying a hydrodynamic distance across of 188.0 nm (SD= 117.7). The polydispersity index was 0.246 and the Zeta-potential value was - 17.2 mV, which indicates good colloidal stability. Results of the Transmission electron microscope (TEM) observation indicated that the particles were spherical in shape with an average size of 21.8- 27.5 nm. The antibacterial efficacy of the AgNPs against Methicillin resistant *Staph. aureus* (MRSA) and *E. coli* clinical isolates was evaluated *in vitro* using the agar well diffusion. The AgNPs demonstrated antibacterial potential against MRSA and *E. coli* isolates; recording 18 and 15 mm diameter of zones of inhibition, respectively. The minimum inhibitory concentration (MIC) was found to be 142 µg/ ml, while the recorded minimum bactericidal concentration (MBC) was 284 µg/ ml. The mode of action of the AgNPs was investigated using the Scanning electron microscope (SEM), which was recognized as bacterial cell lysis and elongation. Current data suggest an efficient biosynthesis of stable AgNPs by *B. subtilis* with remarkable antibacterial potential.

Keywords: *Bacillus subtilis*, Biosynthesis, Silver nanoparticles, MRSA, *E. coli*



Copyright policy

NRMJ allows the author(s) to hold the copyright, and to retain publishing rights without any restrictions. This work is licensed under the terms and conditions of the Creative Commons Attribution (CC BY) license (<https://creativecommons.org/licenses/by/4.0/>)

1. Introduction

Methicillin-resistant *Staph. aureus* (MRSA) is known as a serious causal agent of nosocomial infections that spreads worldwide, and has a negative impact on the patient's health resulting in huge increases in the health care costs ([Luteijn *et al.*, 2011](#)). *Staph. aureus* acquires methicillin resistance by insertion of staphylococcal cassette chromosome (SCCmec) carrying the *mecA* gene into the microbial genome. This gene encodes for penicillin-binding protein PBP-2a, which is not inhibited by the pre-existing β -lactams antibiotics ([Makgotlho *et al.*, 2009](#)).

In recent years, nanotechnology has been of great interest due to its high impact in several fields such as; energy, medicine, electronics and space industries. Medical applications of biosynthesized AgNPs have already started including; targeted drug delivery, cancer treatment, gene therapy and DNA analysis, antibacterial agents, biosensors and enhancers of reaction rates.

Many microbes such as bacteria, fungi, actinobacteria and yeasts are capable of intra-cellular or extra-cellular biosynthesis of NPs, mineral crystals and metallic NPs ([Li *et al.*, 2011](#)). In addition, the most widely used type of nanoparticles is the AgNPs; manipulated as novel therapeutic agents due to their antibacterial; antifungal, antiviral and anti-inflammatory potencies.

Metallic nanoparticles have become of high importance due to their application in many fields, especially when being synthesized in an environmentally safe and inexpensive way. There are numerous microorganisms possessing the ability to synthesize NPs ([Pantidos and Horsfall, 2014](#)), as they have the ability to reduce the Ag^+ to AgNPs ([Fayaz *et al.*, 2010](#)). The previous work of [Panacek *et al.*, \(2006\)](#) revealed that AgNPs have effective antimicrobial activity against both of Gram-positive and Gram-negative bacteria; including the highly multi-resistant strains such as MRSA.

During the current work, the ability of *B. subtilis* strain to cause extracellular synthesis of AgNPs using 1 mM AgNO_3 as a precursor solution was demonstrated. These biosynthesized AgNPs exhibited the power to counteract the clinical strains of *E. coli* and *Staph. aureus*. The objectives of this study were to investigate the ability of *B. subtilis* to synthesis AgNPs, and to test the antibacterial efficacy of the biosynthesized AgNPs against *E. coli* and MRSA.

2. Materials and methods

2.1. Clinical standard strains and bacterial isolates

2.1.1. Standard bacterial strains

In this study, *B. subtilis* ATCC (6633), *E. coli* ATCC (8739) and *Staph. aureus* ATCC (6538) were kindly provided by Microbiology department, Egyptian Drug Authority (EDA), Giza, Egypt.

2.1.2. Collection and identification of the clinical bacterial isolates

During a 12-month period (July, 2017 - 1 July, 2018), clinical bacteria were isolated from different patient's wounds and urine samples; recovered from a total of 96 male and female patients of varying ages, administered to the Microbiology Laboratories of El Kasr El Aini hospital, Cairo, Egypt. Identification of these bacterial isolates was carried out using Gram staining and several standard biochemical reactions including; catalase assay, coagulase assay, DNase test, Mannitol utilization, Lactose fermentation and growth on a number of specific media such as; Eosin methylene blue agar, Triple sugar ion agar and Simmon citrate agar ([Bergey and Holt, 2000](#)). After that, Vitek 2 identification system was manipulated using ID-Gram Positive Cocci cards (ID-GP cards; bioMe'rieux) and ID -Gram Negative cards (ID-GN cards; bioMe'rieux), according to the manufacturer's instructions ([Wattal and Oberoi, 2016](#)).

2.2. Antibiotic susceptibility assay

The recovered *Staph. aureus* and *E. coli* isolates were tested for their antibiotic sensitivity using two antibiotic disks mainly: ceftazidime (CAZ: 30 µg); cefoxitin (FOX: 30 µg); in addition to amikacin (AK: 30 µg); streptomycin (S: 10 µg); tetracycline (TE: 30 µg); amoxicillin/clavulanic acid (AMC: 30 µg); meropenem (MEM: 10 µg); ofloxacin (OFX: 5 µg) and trimethoprim-sulfamethoxazole (STX: 25 µg) for phenotypic detection of MRSA, according to Kirby-Bauer agar disc diffusion assay of [Bauer *et al.*, \(1966\)](#). Results were evaluated following the criteria of the [Clinical and Laboratory Standards Institute \(CLSI\), \(2017\)](#).

2.3. Detection of *mecA* gene for MRSA by Polymerase chain reaction (PCR)

The presence of *mecA* gene was detected in *Staph. aureus* isolates that were recorded to be resistant to cefoxitin, through amplifying a 293-bp fragment using primer pair *mecA* forward (5'-ACGAGTAGATGCTCAATATAA-3') and *mecA* reverse (5'-CTTAGTTCTTTAGCGATTGC3'), in reference to [Sabet *et al.*, \(2007\)](#). The chromosomal DNA was prepared from overnight cultures of the bacterium grown on Brain Heart Infusion (BHI) broth. DNA amplification was carried out in a PCR thermocycler with the following thermal cycling profile: initial denaturation at 94°C for 3 min. followed by 30 sec. at 94 °C, 30 sec. at 60 °C and 30 sec. at 72 °C. Denaturation, annealing and extension were performed in 30 cycle followed by an extra-cycle of annealing at 60 °C for 30 sec., and a final extension at 72 °C for 5 min. A volume of 2 µl of prepared DNA was added to a final volume of 25 µl PCR mixture containing: 12.5 µl Master Mix (Biomatik, Canada), 1 µl of each primer and 8.5 µl of sterile dist. water. The amplified products were visualized by electrophoresis, with UV in 2 % agarose gels stained with Ethidium bromide.

2.4. Extracellular biosynthesis of AgNPs

In this study, *B. subtilis* ATCC (6633) was grown in 250-ml Erlenmeyer flask containing 100 ml Luria-Bertani broth (LB) medium for 36 h at 37 °C with shaking at 150 rpm. After incubation, the culture was centrifuged at 5,000 rpm for 30 min., and then the supernatant was collected to be used as the starting material for extracellular synthesis of AgNPs. Afterwards, 1 mM of AgNO₃ (1% v/v) was added to *B. subtilis* supernatant (pH adjusted to 8.5), and then incubated with shaking at 40 °C (200 rpm) for 5 d under dark conditions ([Sunkar and Nachiyar, 2012](#)). An un-inoculated broth medium was used as a control, to check for the role of bacteria in the biosynthesis of NPs.

2.5. Characterization of the biosynthesized AgNPs

2.5.1. Particle sizing measurements

Particle size analysis was conducted by means of dynamic light scattering assay (Laser diffractometry) using an extremely compact optical bench; the CILAS 1064 integrates 2 sequenced laser sources pointed at 0° and 45°. Measurements were taken in the range of 0.04-500 µm.

2.5.2. Transmission electron microscope (TEM)

The TEM was used for detection of the NPs size and shape. Samples were prepared by placing a drop of the biosynthesized AgNPs over a gold-coated negative grid followed by evaporation of the solvent ([Germain *et al.*, 2003](#)); using TEM, JEOL-JEM-1011 instrument at 100 kV.

2.5.3. Zeta potential measurement (ZP)

Measurement of ZP was carried out for the AgNPs to detect their colloidal stability, using Malvern Zetasizer Nano ZS analyzer at room temperature (Zetasizer Nano-ZS-instrument, Worcestershire, United Kingdom), in reference to [Elbeshehy *et al.*, \(2015\)](#).

2.6. Detection of the *in vitro* antibacterial potential of the AgNPs

The agar well diffusion assay was used to evaluate the *in vitro* antibacterial efficacy of the biosynthesized AgNPs, according to [Singh *et al.*, \(2013\)](#). A single colony of the tested *B. subtilis* was picked up, inoculated into MH broth and then incubated overnight at 37 °C. The OD of the bacterial suspension was adjusted to 0.5 McFarland ($\approx 1 \times 10^8$ cfu/ ml); a loopful of this suspension was inoculated into Mueller Hinton agar (MHA) medium, and then poured into Petri plates. A 50 μ l of 1mM of AgNPs solution was added to the center of each well (10 mm), which were punched in the MHA plates using a sterile cork borer. Control sample was made using either 50 μ l of the sterile supernatant derived from *B. subtilis* culture or 1mM of AgNO₃ solution; instead of the tested AgNPs. After incubation at 37 °C for 24 h, the zones of inhibition were measured using a calibrated ruler. The assay was performed in triplicates, and repeated two times.

2.7. Evaluation of the minimum inhibitory concentration (MIC) and minimum bactericidal concentration (MBC) of the AgNPs

The MIC of the AgNPs was determined through the two-fold broth dilution method using the MHB following the criteria of [CLSI. \(2017\)](#). From a stock suspension of 1mM of the biosynthesized AgNPs; two-fold serial dilutions were prepared using MHB. Bacterial isolates, in their exponential growth phase; were inoculated in the wells of a 96-microwell plate containing either MHB alone as a positive control, or MHB containing the biosynthesized AgNPs at a final concentration ranging from 17.75- 568 μ g/ ml. The microplate was then incubated at 37 °C for 24 h. The MIC corresponded to the AgNPs concentration that inhibited the bacterial growth, compared to the positive control. On the other hand, MBC was determined by sub-culturing the contents of the clear wells that showed no growth in the MIC assay onto MHA plates. The assays were performed in triplicates, and repeated two times.

2.8. Morphological changes in the bacterial cells

Morphological changes in shapes of the bacterial strains i.e. *Staph. aureus* and *E. coli* treated with the biosynthesized AgNPs were observed using Scanning electron microscopy (SEM) (JEOL, JSM-5200 LV SEM, Japan); with the voltage set to 25 kV at 5,000 \times magnification power, according to [Chakravarty and Banerjee, \(2008\)](#). The isolates were incubated individually overnight with sub-inhibitory concentration of the AgNPs. At the end of incubation, morphological changes in the bacterial cells treated with AgNPs were observed under SEM, compared to the untreated control cells.

2.9. Statistical analysis

The significance of the antibacterial potency of the AgNPs was checked by standard variance of analysis (ANOVA). *p* values < 0.05 were considered significant. The mean values \pm SD (standard deviation) were presented. The data was analyzed with Graph Pad Prism 7.

3. Results

3.1. Isolation and identification of the clinical bacterial isolates

In this study, about 50 isolates of *Staph. aureus* and 46 isolates of *E. coli* were recovered from patients of El Kasr El Aini Hospital, Microbiology laboratories, Egypt. Species-level identification of the isolates was confirmed using the biochemical profile and VITEK 2 system; with confidence levels of 93-95 % probability.

3.2. Antibiotic susceptibility pattern

Results showed that *Staph. aureus* isolates were resistant to amoxicillin/clavulanic acid by 100 %, and presented much lower resistance towards trimethoprim-sulfamethoxazole by 34 %, as demonstrated in Fig. (1). As demonstrated in Fig. (2), *E. coli* isolates were found to be resistant to ceftazidime by 94 %, with much lower resistance to Amikacin by 24 %.

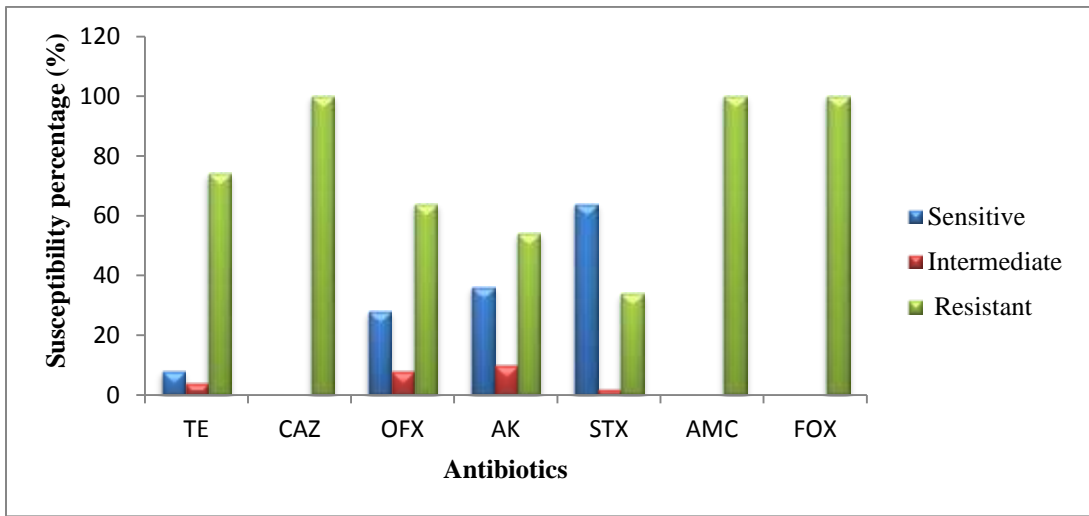


Fig. 1: Antibiotic susceptibility pattern of *Staph. aureus*, demonstrating different sensitivity to the various tested antibiotics

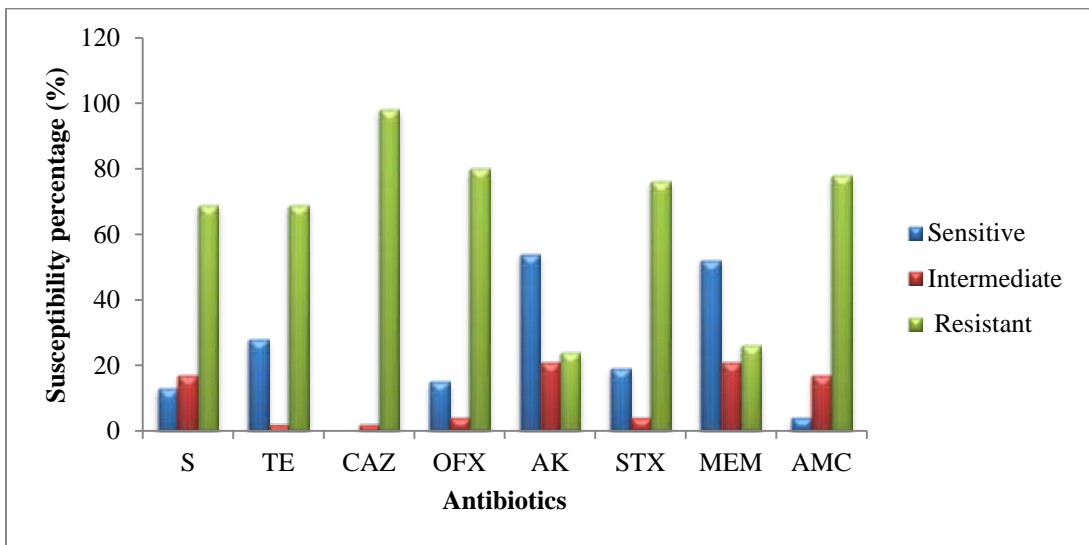


Fig. 2: Antibiotic susceptibility pattern of *E. coli*, demonstrating different sensitivity to the various tested antibiotics

3.3. Detection of *mecA* gene in the MRSA isolate

Further identification of the *Staph. aureus* isolates that expressed resistance to ceftiofur, and phenotypically identified as MRSA, through detection

of the *mecA* gene in these isolates using PCR assay. Results showed that 62 % (31/50) of *Staph. aureus* isolates possessed *mecA* gene Fig. (3).

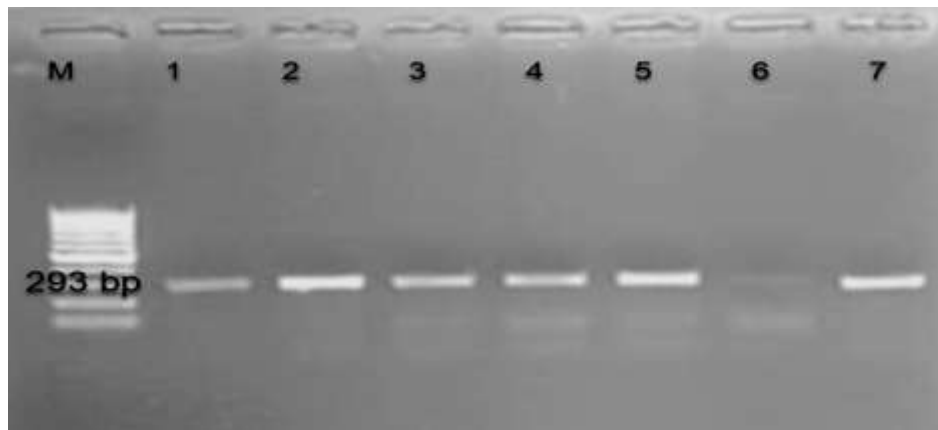


Fig. 3: Agarose gel electrophoresis of PCR product obtained from the MRSA isolates. Where; Lane M: marker 100 bp ladder, Lane 1, 2, 3, 4, 5 and 7: positive *mecA* gene, Lane 6: negative *mecA* gene

3.4. Biosynthesis of AgNPs using supernatant of *B. subtilis*

Supernatant collected from *B. subtilis* LB culture used as the starting material for extracellular synthesis of AgNPs, turned the color of the treated AgNO_3

solution from pale yellow to reddish brown (Fig. 4a, b). This finding indicated the formation and deposition of AgNPs, while the color of AgNO_3 solution (negative control) remained unchanged.

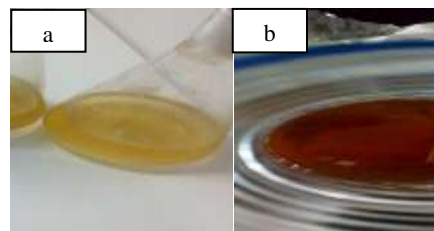


Fig. 4: (a) Supernatant culture of *B. subtilis* before incubation with the AgNO_3 solution (yellow), and (b) supernatant culture of *B. subtilis* after incubation with AgNO_3 (brown), indicating the formation of AgNPs

3.5. Physical characterization of AgNPs

Samples of AgNPs were subjected to TEM analysis for characterization. Results revealed that the AgNPs were spherical in shape with particle size diameter of 21.8- 27.5 nm, as demonstrated in Fig. (5). The size distribution and zeta potential of AgNPs were determined by dynamic light scattering and

Zetasizer analyzer, respectively. Results in Fig. (6) demonstrates that the Z-Average (d. nm) was 135.0 nm; with 99.2 % of the particles exhibiting a hydrodynamic diameter of 188.0 nm (SD= 117.7). The polydispersity index was 0.246 and the zeta-potential (ZP) value was -17.2 mV, which indicates good colloidal stability of the AgNPs.



Fig. 5: TEM micrograph at 20,000 times magnification recorded from a drop-coated film of an aqueous solution of AgNPs, showing the spherical shape of the particles and their average diameter of 21.8- 27.5 nm

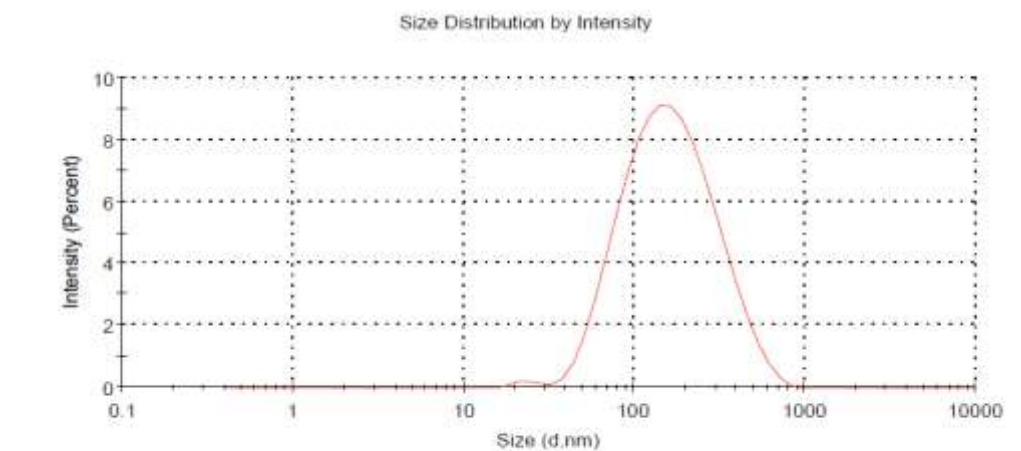


Fig. 6: Size distribution intensity graph of biosynthesized AgNPs, demonstrating Z-Average (d. nm) of 135.0

3.6. Antibacterial efficacy of the AgNPs

Preliminary screening of the in vitro antibacterial potential of the AgNPs was assessed against 77 clinical isolates (31 MRSA and 46 *E. coli*), in addition to the control standard strains of *E. coli* ATCC (8739) and *Staph. aureus* ATCC (6538); using the agar well diffusion. The obtained data presented in Table (1) and

Fig. (7) show the inhibitory activity of AgNPs against MRSA and *E. coli* isolates; recording diameter of zones of inhibition of 18, 15 mm, respectively. These clearly indicate that the difference in the inhibitory action of the AgNPs on the tested bacterial spp. was statistically significant ($p < 0.05$), compared to the control wells that showed no inhibition zones.

Table 1: Antibacterial potency of biosynthesized AgNPs, 1mM AgNO₃ and *B. subtilis* culture supernatant against clinical and standard bacterial isolates

Clinical / Standard isolates	Mean zone of inhibition \pm SD (in mm)		
	Biosynthesized AgNPs (1 mM)	AgNO ₃ (1 mM)	<i>B. subtilis</i> culture supernatant
MRSA	18 \pm 1.387	10.7 \pm 0.763	0
<i>E. coli</i>	15 \pm 1.201	10.5 \pm 0.863	0
<i>E. coli</i> ATCC (8739)	17 \pm 0.112	11 \pm 0.101	0
<i>Staph. aureus</i> ATCC (6538)	19 \pm 0.121	10 \pm 0.112	0

Where; Data were expressed through measurement of diameter of inhibition zones as means of three replicates in mm \pm SD, * p -value was significant < 0.05

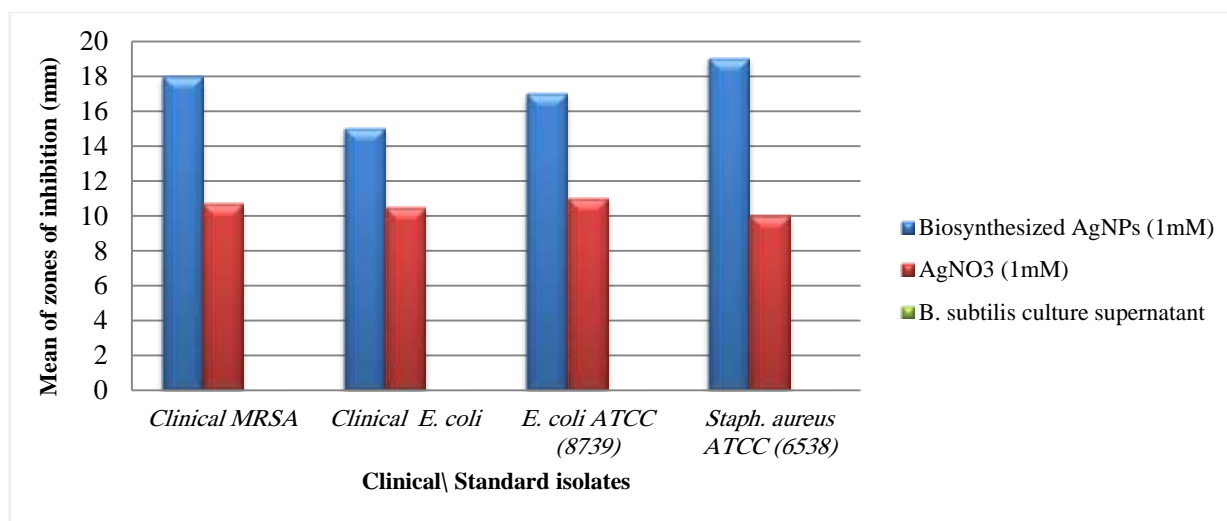


Fig. 7: Antibacterial efficacy of biosynthesized AgNPs (1 mM), AgNO₃ (1 mM) and *B. subtilis* culture supernatant against the clinical and standard bacterial isolates

3.7. The MIC and MBC of the biosynthesized AgNPs

The MIC and MBC values of the biosynthesized AgNPs against the tested microbial isolates were determined. The recorded MIC was 142 $\mu\text{g}/\text{ml}$, while the MBC was 284 $\mu\text{g}/\text{ml}$, as presented in Table (2). The MIC and MBC indicated massive antibacterial effectiveness of the AgNPs.

3.8. Morphological changes in shapes of the AgNPs treated bacterial cells

Results of SEM indicated that the non-treated bacterial cells were intact without any noticeable damage; while upon interaction with the AgNPs, the bacterial cells were damaged that was observed as cell lysis of *Staph. aureus* and cell elongation of *E. coli*. (Fig. 8).

Table 2: The MIC and MBC of the biosynthesized AgNPs against the clinical and the standard bacterial isolates

Clinical / Standard isolates	MIC ($\mu\text{g}/\text{ml}$)	MBC ($\mu\text{g}/\text{ml}$)
MRSA	142	284
<i>E. coli</i>	142	284
<i>E. coli</i> ATCC (8739)	35.5	70
<i>Staph. aureus</i> ATCC (6538)	35.5	70

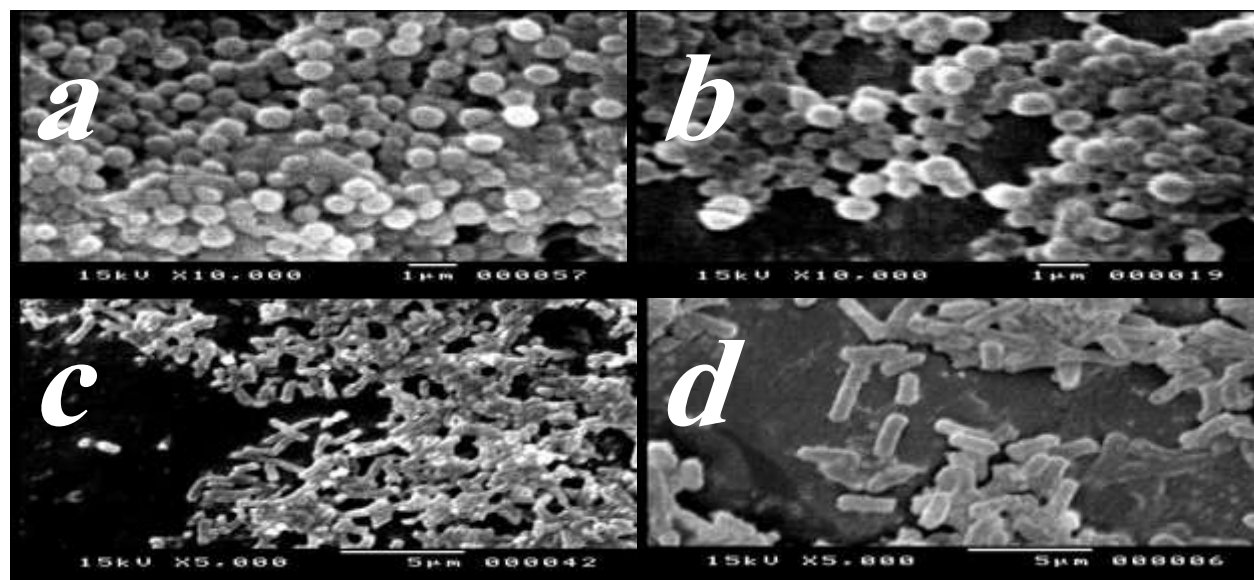


Fig. 8: Scanning electron micrographs of (a): control *Staph. aureus* cells, (b): AgNPs treated *Staph. aureus* cells (c): control *E. coli* cells and (d): AgNPs treated *E. coli* cells, demonstrating cell lysis and cell elongation of *Staph. aureus* and *E. coli*, respectively

4. Discussion

Currently, MRSA is a major cause of morbidity and mortality worldwide ([de Kraker *et al.*, 2011](#)). There are several antimicrobial susceptibility testing assays used for detection of MRSA including; oxacillin screening test, oxacillin and/or ceftoxitin disk diffusion method and oxacillin MIC test, as highlighted by [Tubbicke *et al.*, \(2012\)](#). Current results revealed that the tested *Staph. aureus* isolates were 100 % resistant to ceftoxitin, so these isolates were phenotypically identified as MRSA. These conventional antimicrobial tests used for MRSA identification were always associated with false negative and positive results. Therefore, it is necessary to use PCR for microbial identification, which is considered as a DNA-based assay. Our results demonstrated that only 62 % (31/50) of *Staph. aureus* isolates possessed *mecA* gene; however, there is no *mecA* gene detected in methicillin-sensitive *Staph. aureus* (MSSA) strains. A previous study conducted by [Hallin *et al.*, \(2003\)](#) reported that detection of this gene in any strains of *Staph. aureus* is indicative of MRSA.

Synthesis of AgNPs is accompanied with significant modifications of the properties of metals; owing to their extremely small size and high surface area to volume ratio. Moreover, [Mohd Yusof *et al.*, \(2019\)](#) added that NPs exhibit distinctive characteristics that led to significant differences in their properties compared to the bulk counterparts.

Usually, AgNPs synthesis is detected through a color change of the reaction mixture from yellow to dark brown ([Karbasiyan *et al.*, 2008](#)), so appearance of brown color indicates the formation of AgNPs, which is in accordance with the results of this study. A previous work of [Yamal *et al.*, \(2013\)](#) attributed this color change to the surface plasma resonance property of the NPs. The antibacterial potency of AgNPs increased considerably with the decrease in the particles size. [Dauthal and Mukhopadhyay \(2016\)](#)

stated that low particles size is useful for successful delivery of the targeted drugs, which comply with the current detected particle size of the biosynthesized AgNPs that ranged from of 21.8- 27.5 nm. In a previous study conducted by [Cho *et al.*, 2005](#)), (it was proved that high surface area to volume ratio of the AgNPs causes high bactericidal efficacy compared to the bulk silver metal. Accordingly, the biosynthesized AgNPs are considered as promising therapeutic agents that demonstrate significant antimicrobial activities.

An early study conducted by [Saifuddin *et al.*, \(2009\)](#) revealed that AgNPs biosynthesized by reaction of Ag⁺ ions with *B. subtilis* culture supernatant is exceptionally stable, which is likely attributed to capping with proteins secreted by the bacteria. In addition, Zeta potential of the biosynthesized AgNPs indicated their stability; which is also attributed to the presence of microbial proteins that cover the NPs. This coincides with the current results recording a zeta-potential value of -17.2 mV.

The antibacterial efficacy of AgNPs is attributed to different possible mechanisms of action. [Marambio-Jones and Hoek, \(2010\)](#) believed that the positive charged silver ions (Ag⁺) of AgNPs becomes attached to the negatively charged cell surface causing disturbance in its physical and chemical properties, which in turn disturb the membrane functions including; permeability, electron transport and respiration. [Rajeshkumar and Malarkodi, \(2014\)](#) proposed another possible mode of action stating that AgNPs can interact with the microbial cells leading to inhibition of their respiratory chain enzymes and increasing the cells permeability to phosphate and protons; through altering trans-membrane electron transfer. Furthermore, AgNPs may cause damage to the bacterial cells in consequence of the interaction with the proteins, DNA and other sulfur- and phosphorus-containing cell constituents, as reported by [Nayak *et al.*, \(2015\)](#). This is the nearest mode of action of AgNPs that our current results comply with, where

cell lysis of *Staph. aureus* and cell elongation in *E. coli* were observed upon treatment with AgNPs.

Conclusion

In this study, the ability for extracellular biosynthesis of AgNPs using 1 mM AgNO₃ as a precursor solution was demonstrated by the *B. subtilis*. The AgNPs had the power to counteract with clinical isolates of *E. coli* and *Staph. aureus*. TEM analysis revealed the spherical shape of AgNPs with particle size of 20- 47 nm. Zeta potential analysis presented a value of -17.2 mV, which expresses the colloidal stability of the AgNPs. Such NPs have been found to be effective against different drug-resistant bacterial strains that were pathogenic, and these findings were confirmed through SEM analysis. The possible antibacterial activity of AgNPs against the different pathogens was confirmed during this study.

Acknowledgements

The authors appreciate the support provided by the Egyptian Drug Authority (EDA), Formerly National Organization for Drug Control and Research (NODCAR), Giza, Egypt.

Conflict of interest

The authors declare that they have no conflicts of interest related to the work done in this manuscript.

Funding source

This study did not receive any fund.

Ethical approval

Non-applicable, as no *in vivo* studies were carried out.

5. References

Bauer A.W.; Kirby W.M.; Sherris J.C. and Turck, M. (1966). Antibiotic susceptibility testing by a standardized single disk method. *American Journal of Clinical Pathology*. 45(4): 493-496.

Bergey, D.H. and Holt, J.G. (2000). *Bergey's Manual of Determinative Bacteriology*, Philadelphia Lippincott Williams and Wilkins.

Chakravarty, R. and Banerjee, P.C. (2008). Morphological changes in an acidophilic bacterium induced by heavy metals. *Extremophiles*. 12(2): 279-284.

Cho, K.H.; Park, J.E.; Osaka, T. and Park, S.G. (2005). The study of antimicrobial activity and preservative effects of nanosilver ingredient. *Electrochimica Acta*. 51(5): 956-960.

Clinical and Laboratory Standards Institute (CLSI). (2017). Performance Standards for Antimicrobial Susceptibility Testing, in 27th Edition. CLSI supplement M100, Wayne, PA: Clinical and Laboratory Standards Institute.

Dauthal, P. and Mukhopadhyay, M. (2016). Noble metal nanoparticles: plant-mediated synthesis, mechanistic aspects of synthesis, and applications. *Industrial and Engineering Chemistry Research*. 55: 9557-9577.

De Kraker, M.E.; Wolkewitz, M.; Davey, P.G.; Koller, W.; Berger, J.; Nagler, J. et al. (2011). Clinical impact of antimicrobial resistance in European hospitals: excess mortality and length of hospital stay related to methicillin-resistant *Staphylococcus aureus* bloodstream infections. *Antimicrobial Agents and Chemotherapy*. 55(4): 1598-1605.

Elbeshehy E.K.; Elazzazy A.M., and Aggelis, G. (2015). Silver nanoparticles synthesis mediated by new isolates of *Bacillus* spp., nanoparticle characterization and their activity against Bean Yellow Mosaic Virus and human pathogens. *Frontiers in Microbiology*. 6: 453.

Fayaz, A.M.; Balaji, K.; Girilal, M.; Yadav, R.; Kalaichelvan, P.T. and Venketesan, R. (2010). Biogenic synthesis of silver nanoparticles and their synergistic effect with antibiotics: a study against

Gram-positive and Gram-negative bacteria. *Nanomedicine*. 6(1): 103-109.

Germain, V.; Li, J.; Inger, D.; Wang, Z.L. and Pileni, M.P. (2003). Stacking faults in formation of silver nano-disks. *Journal of Physical Chemistry B*. 107: 8717-8720.

Hallin, M.; Maes, N.; Byl, B.; Jacobs, F.; De Gheldre, Y. and Struelens, M.J. (2003). Clinical impact of a PCR assay for identification of *Staphylococcus aureus* and determination of methicillin resistance directly from blood cultures. *Journal of Clinical Microbiology*. 41(8): 3942-3944.

Karbasian, M.; Atyabim, S.; Siyadat, S.; Momen, S. and Norouzi, D. (2008). Optimizing nanosilver formation by *Fusarium oxysporum* PTCC 5115 employing response methodology. *American Journal of Agricultural and Biological Sciences*. 3: 433-437.

Li, X.; Xu, H.; Chen, Z.S. and Chen, G. (2011). Biosynthesis of Nanoparticles by Microorganisms and Their Applications. *Journal of Nanomaterials*. 1-16.

Luteijn, J.M.; Hubben, G.A.; Pechlivanoglou, P.; Bonten, M.J. and Postma, M.J. (2011). Diagnostic accuracy of culture-based and PCR-based detection tests for methicillin-resistant *Staphylococcus aureus*: a meta-analysis. *Clinical Microbiology and Infection*. 17(2): 146-154.

Makgotlho, P.E.; Kock, M.M.; Hoosen, A.; Lekalakala, R.; Omar, S.; Dove, M. and Ehlers, M.M. (2009). Molecular identification and genotyping of MRSA isolates. *FEMS Immunology and Medical Microbiology*. 57(2): 104-115.

Marambio-Jones, C. and Hoek, E.M.V. (2010). A review of the antibacterial effects of silver nanomaterials and potential implications for human health and the environment. *Journal of Nanoparticle Research*. 12(5): 1531-1551.

Mohd Yusof, H.; Mohamad, R.; Zaidan, U.H. and Abdul Rahman, N.A. (2019). Microbial synthesis of zinc oxide nanoparticles and their potential application as an antimicrobial agent and a feed supplement in animal industry: A review. *Journal of Animal Science and Biotechnology*. 10: 57.

Nayak, B.K.; Chitra, N. and Nanda, A. (2015). Comparative antibiogram analysis of AgNPs synthesized from two *Alternaria* spp. with amoxicillin antibiotics. *Journal of Chemical and Pharmaceutical Research*. 7: 727-731.

Panacek, A.; Kvítek, L.; Pucek, R.; Kolar, M.; Vecerova, R.; Pizúrova N. et al. (2006). Silver colloid nanoparticles: synthesis, characterization, and their antibacterial activity. *Journal of Physical Chemistry B*. 110(33): 16248-16253.

Pantidos, N. and Horsfall, L.E. (2014). Biological Synthesis of Metallic Nanoparticles by Bacteria, Fungi and Plants. *Nanomedicine and Nanotechnology*. 5(5): 233-242.

Rajeshkumar, S. and Malarkodi, C. (2014). *In Vitro* Antibacterial Activity and Mechanism of Silver Nanoparticles against Foodborne Pathogens. *Bioinorganic Chemistry and Applications*. 5881-5890.

Sabet, N.S.; Subramaniam, G.; Navaratnam, P. and Sekaran, S.D. (2007). Detection of *mecA* and *ermA* genes and simultaneous identification of *Staphylococcus aureus* using triplex real-time PCR from Malaysian *Staph. aureus* strain collections. *International Journal of Antimicrobial Agents*. 29(5): 582-585.

Saifuddin, N.; Wong, C.W. and Nur Yasumirsa, A.A. (2009). Rapid Biosynthesis of Silver Nanoparticles Using Culture Supernatant of Bacteria with Microwave Irradiation. *E-Journal of Chemistry*. 6(1): 61-70.

Singh, R.; Wagh, P.; Wadhvani, S.; Gaidhani, S.; Kumbhar, A.; Bellare J. et al. (2013). Synthesis, optimization, and characterization of silver

nanoparticles from *Acinetobacter calcoaceticus* and their enhanced antibacterial activity when combined with antibiotics. *International Journal of Nanomedicine*. 8: 4277-4290.

Sunkar, S. and Nachiyar, C.V. (2012). Biogenesis of antibacterial silver nanoparticles using the endophytic bacterium *Bacillus cereus* isolated from *Garcinia xanthochymus*. *Asian Pacific Journal of Tropical Biomedicine*. 2(12): 953-959.

Tubbicke, A.; Hubner, C.; Kramer, A.; Hubner, N.O. and Flessa, S. (2012). Transmission rates, screening methods and costs of MRSA-a systematic literature review related to the prevalence in Germany. *European Journal of Clinical Microbiology and Infectious Diseases*. 31(10): 2497-2511.

Wattal, C. and Oberoi, J.K. (2016). Microbial identification and automated antibiotic susceptibility testing directly from positive blood cultures using MALDI-TOF MS and VITEK 2. *European Journal of Clinical Microbiology and Infectious Diseases*. 35(1): 75-82.

Yamal, G.; Sharmila, P.; Rao, K.S. and Pardha, S. (2013). Inbuilt potential of YEM medium and its constituents to generate Ag/Ag₂O nanoparticles. *PLOS ONE*. 8(4): e61750.